

## I. ELECTRON-PROTON ELASTIC SCATTERING

### A. Introduction

Studies of electron-proton scattering<sup>(1)</sup> have been previously carried out at linear accelerators and electron synchrotrons in order to obtain information about the structure of the proton. Because of limitations in energy and beam intensities these measurements were able to determine separately the electric and magnetic form factors of the proton,  $G_E$  and  $G_M$ , only up to squared four-momentum transfers,  $q^2$ , of about  $2 \text{ (BeV/c)}^2$ . CEA experiments at higher  $q^2$  values have placed a limit of about 0.04 on  $G_E$ , and  $G_M$  has been determined to an accuracy of about 0.02.<sup>(1)</sup> Utilizing the higher intensities and energies available at SLAC, we expect to extend considerably the measurements of the form factors to higher four-momentum transfers. Figure 1 shows the range of four-momentum transfers available at SLAC. The maximum value is about  $37 \text{ (BeV/c)}^2$  corresponding to an incident energy of 20 BeV. Since the form factors decrease rapidly as  $q^2$  increases, the range over which these measurements can be extended depends critically on the detailed behavior of the form factors. However it is useful to list some of the questions of interest that can be investigated by extending the measurements to higher  $q^2$ :

- (1) Existence of a nucleon core.
- (2) Validity of the pole description of nucleon form factors.
- (3) Validity of the Wu and Yang form factor,<sup>(2)</sup> that  $G \sim e^{-|q|/0.6}$ .
- (4) Hypothesis of Drell<sup>(3)</sup> that  $G > e^{-|q|/2M}$ .
- (5) Hypothesis of Sachs<sup>(4)</sup> that  $G_E = G_M$  at large  $q^2$ .
- (6) Hypothesis that  $F_2(q^2)$  and  $F_1(q^2)/q^2$  asymptotically approach zero as  $q^2$  becomes large.<sup>(6)</sup>

Aside from shedding light on the validity of the above hypotheses, determinations of the detailed behavior of the proton form factors at large  $q^2$  will provide very valuable constraints and guide posts to any future theory of the nucleon and its interactions with other particles.

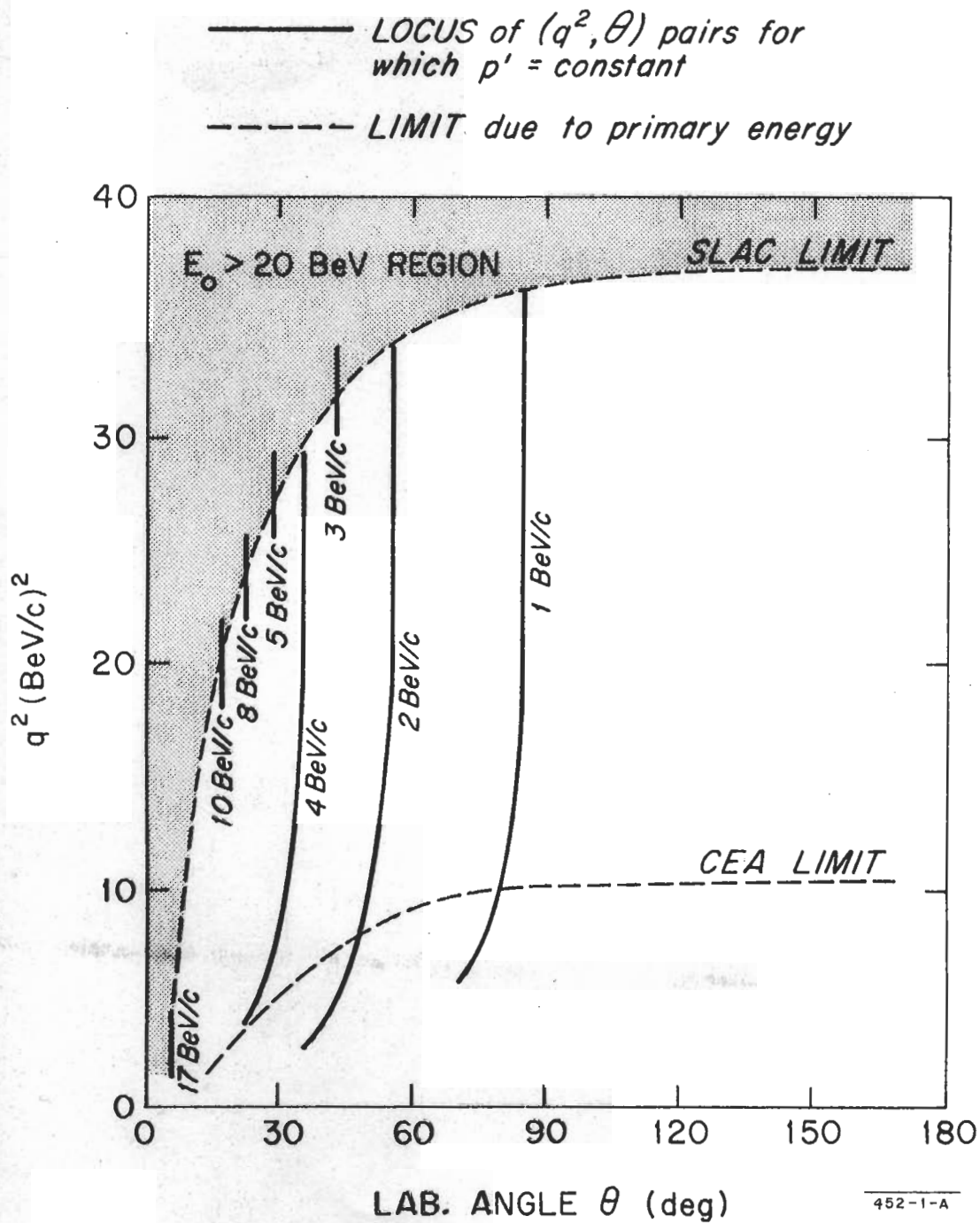


**FIG. 1 - FOUR-MOMENTUM TRANSFER SQUARED VALUES AVAILABLE AT SLAC.**

## B. Rosenbluth Cross Section and Its Validity

Assuming the validity of the first order Born approximation (one-photon exchange) the cross section for electron-proton elastic scattering is given by the Rosenbluth formula :

$$\frac{d\sigma}{d\Omega} = \sigma_{NS} \left( \frac{G_E^2 + \tau G_M^2}{1 + \tau} + 2\tau G_M^2 \tan^2 \frac{\theta}{2} \right)$$

where

$$\sigma_{NS} = \left( \frac{m_e r_e}{2E_0 \sin^2 \frac{\theta}{2}} \right)^2 \frac{E'}{E_0} \cos^2 \frac{\theta}{2}$$

$$\tau = \frac{q^2}{4M^2}, \quad q^2 = 2E_0 E' (1 - \cos \theta)$$

in which

$E_0$  = incident electron energy

$E'$  = scattered electron energy

$\theta$  = scattering angle

$r_e$  = classical radius of the electron = 2.82 fermi

$m_e$  = electron mass

$M$  = proton mass

Electron-proton elastic scattering data have been analyzed in terms of a one-photon exchange process, and the results have been consistent with this point of view. However, a series of experiments comparing electron and positron scattering from the proton at incident energies up to 850 MeV and four-momentum transfers squared up to  $0.76 (\text{BeV}/c)^2$  have indicated<sup>(5)</sup> that small deviations may be present. In order to interpret properly the electron-proton elastic scattering results of this program the deviations from the first Born approximation will have to be determined. This can be done in a number of ways:

- (1) By comparing electron and positron scattering from the proton.



- (2) By investigating the angular distribution of electron-proton elastic scattering at constant  $q^2$ .
- (3) By measuring the polarization of the recoil protons from the scattering process.

Method (1) will be discussed in Part III of this proposal. Method (2) would show up violations of the Rosenbluth formula as deviations from a straight line plot of the data (which is discussed in Section D). This will be checked over the limited number of measurements in the e-p elastic scattering program, but we hope to submit a proposal to perform a detailed search for this effect at a later date using all three spectrometers to cover the complete angular range. Such an experiment will require high accuracy and is thus not suitable to include in this first proposal.

### C. Experimental Requirements

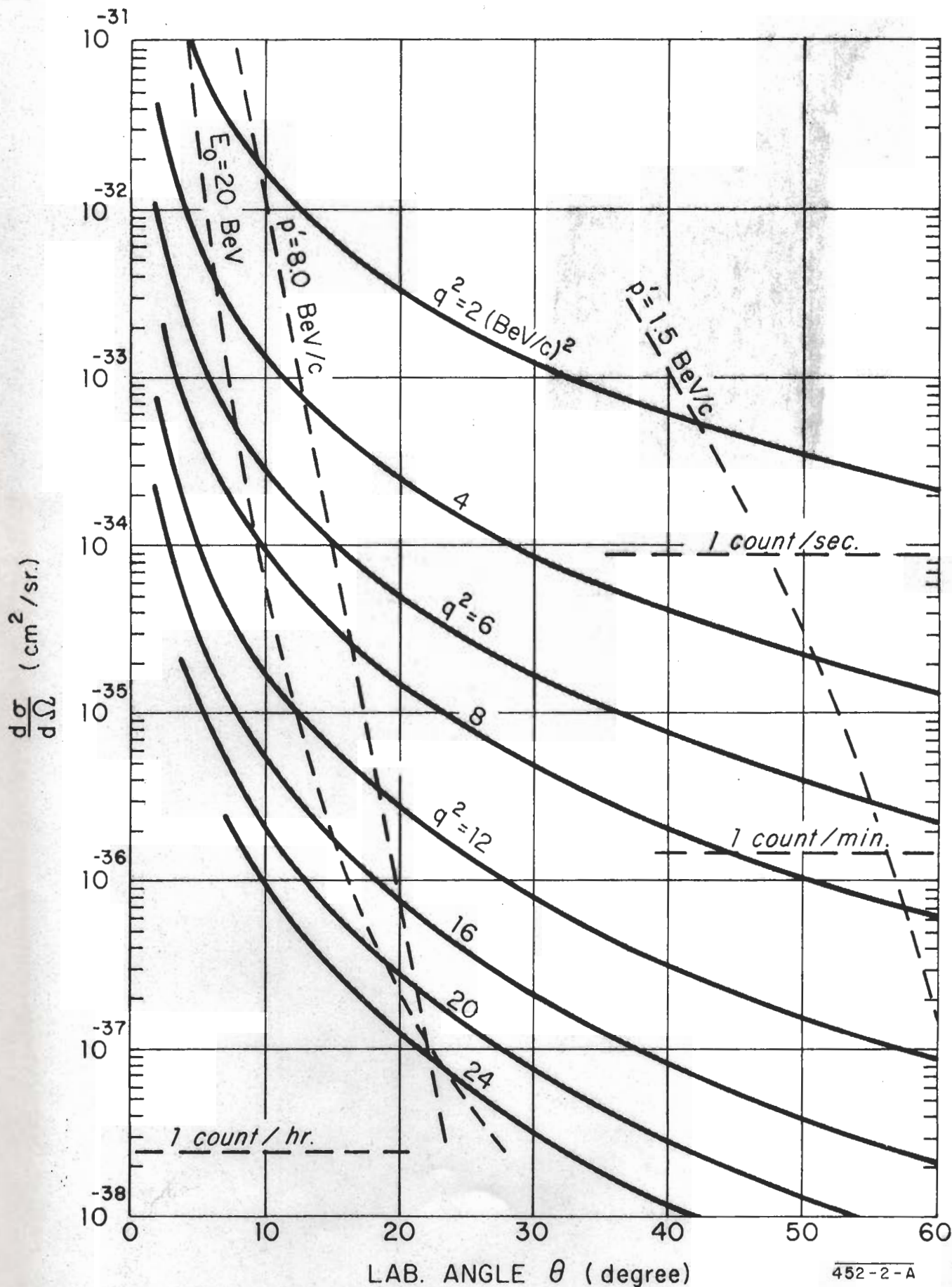
Using the Rosenbluth formula and the recent CEA expressions<sup>(1)</sup> for the form factors we show in Fig. 2 the predicted variation of  $d\sigma/d\Omega$  with  $\theta$  for fixed values of  $q^2$ . The curve of incident energy  $E_0 = 20$  BeV indicates the limit imposed by the machine energy. In this experiment the primary electron beam will strike a 20 cm (0.024 radiation lengths) liquid hydrogen target and the energy spectrum of scattered electrons near the elastic scattering energy will be detected using the 8-BeV/c spectrometer over a range of angles. In Fig. 2 we also show the curve of scattered momentum  $p' = 8.0$  BeV/c and the predicted counting rates assuming an incident beam intensity of  $2 \times 10^{13}$  electrons/sec.

To separate the elastic peak from the pion production threshold in the energy spectrum of the scattered electrons requires a high momentum resolution ( $\approx \pm 0.05\%$ ) spectrometer. This also implies that we will require the following properties of the primary electron beam as it emerges from the Beam Switchyard (BSY):

Absolute energy calibration of BSY :  $1/4 - 1/2\%$  .

Relative energy calibration :  $10^{-3}$  .

Reproducibility of the BSY transport system : Max  $10^{-3}$  ( $10^{-4}$  desirable, as it would save machine time) .



452-2-A

FIG. 2 - PREDICTED  $\frac{d\sigma}{d\Omega}$  vs  $\theta$  USING THE CEA POLE FIT FORM FACTORS.

Energy spread of primary beam	: min $\pm 0.1\%$ .
Beam size	: Height $\lesssim 3$ mm, width $\lesssim 1$ cm.
Stability in position	: $\sim 1$ mm vertically and $\sim 2$ mm horizontally at target.
Beam divergence	: horizontally $\sim 10^{-4}$ rad, vertically $\sim 3 \times 10^{-4}$ rad.
Beam intensity	: Our target is being designed to handle about $5 \mu\text{A}$ ( $3 \times 10^{13}$ electrons/sec). Hopefully we may be able to use more. (At high resolution this is equivalent to $\sim 30 \mu\text{A}$ from the machine.) For the runs at lowest $q^2$ , the intensity at the target must be reduced by factors $\sim 2-50$ .
Beam density outside spot of 2 cm diameter	: $10^{-5}$ of central beam density.
Time structure of current pulse	: We can record one event/pulse, but the accidental rate in the hodoscopes is proportional to the square of the beam intensity. Thus a uniform distribution ( $\pm 15\%$ of flat top) is requested, with the maximum available pulse length.

There may be more complex requirements if there are significant correlations in the beam between  $x$  and  $\theta$ , or  $y$  and  $\phi$ . The quantities  $x$ ,  $y$ ,  $\theta$ ,  $\phi$  are defined in Appendix I.

#### D. Determination of The Proton Form Factors

Present knowledge of the form factors  $G_E$  and  $G_M$  comes mainly from the various measurements done at  $q^2 < 2.0$  (BeV/c)<sup>2</sup>. These experimental data have been numerically fitted with expressions of different forms, such as

$$G_{E,M} = \sum_i \frac{a_i}{\left(1 + \frac{q^2}{b_i}\right)} \quad (\text{pole-fit})$$

$$G_E = \frac{G_M}{\mu} = \frac{1}{\left(1 + \frac{q^2}{0.72}\right)^2} \quad (\text{numerical fit}^{(6)})$$



or even the exponential form

$$G_E = \frac{G_M}{\mu} \sim B e^{-\frac{|q|}{0.6}} \quad (\text{Wu and Yang fit}^{(2)})$$

which falls off much faster as  $q^2$  increases than any other assumed expression. We try to avoid any detailed speculations about the behavior of these form factors at high  $q^2$ .

To separate  $G_E$  and  $G_M$  we will follow the usual procedure of plotting  $(1/\sigma_{NS})(d\sigma/d\Omega)$  against  $\tan^2 \theta/2$  as a straight line for a given constant value of  $q^2$ , assuming the validity of the Rosenbluth relation:

$$\frac{1}{\sigma_{NS}} \left( \frac{d\sigma}{d\Omega} \right) = \left( \frac{G_E^2 + \tau G_M^2}{1 + \tau} + 2 \tau G_M^2 \tan^2 \frac{\theta}{2} \right).$$

The factor  $G_M^2$  is obtained directly from the slope and  $G_E^2$  from the intercept in the ordinate (at  $\theta = 0^\circ$ ). In order to use the data efficiently the measurements will be made at several angles equally spaced in  $\tan^2 \theta/2$  and to approximately equal statistical accuracy on each value of the cross section. Any deviation from the straight line will provide a test of the one-photon exchange assumption, although this would need to be studied in much more detail.

We have made a statistical analysis for minimizing the running time for the experiment. The problem is, given a desired accuracy of the values of  $G_E^2$  and  $G_M^2$ , at what maximum angle of measurement does a minimum in running time occur? Since the cross section drops rapidly as a function of angle, even for constant  $q^2$ , the effects of backgrounds most likely become more severe at larger angles. Thus it would be useful to determine if there is an angle beyond which it is no longer efficient to take data from a statistical standpoint. Thus the objective of this approach is to minimize running time and to see simultaneously whether it is possible to decrease systematic errors due to backgrounds. The detailed analysis is given below in Section H.

We have defined two figures of merit,  $1/MM$  and  $1/ME$ , given by

$$ME \equiv \left( \frac{\delta G_E^2}{G_E^2} \right)^2 \cdot T$$

$$MM \equiv \left( \frac{\delta G_M^2}{G_M^2} \right)^2 \cdot T$$

where  $\delta G_{E,M}^2$  is the error in  $G_{E,M}^2$  and  $T$  is the total running time.

As is shown in Section H, the figures of merit are independent of the total running time and the specific counting errors at each point. In Figs. 3(a-d) we show the variation of  $MM$  and  $ME$  for a range of  $q^2$  from 6.0 to 18.0 (BeV/c)<sup>2</sup>. For these curves the value of the minimum angle at which the cross section is measured has been set at 15°. This is approximately the smallest angle for which the 8-BeV/c spectrometer does not intercept the primary electron beam. We conclude the following from the analysis:

1. **Minima exist both for  $MM$  and  $ME$ .** Figure 4 shows the angles corresponding to  $ME_{\min}$  and  $MM_{\min}$  as a function of  $q^2$  for a five-point fit to a straight line. In Fig. 5 the ranges of  $\theta$  corresponding to  $MM_{\min} < MM < 1.25 MM_{\min}$  and  $ME_{\min} < ME < 1.25 ME_{\min}$  are shown as a function of  $q^2$ . The limits  $1.25 MM_{\min}$  and  $1.25 ME_{\min}$  correspond to a 25 percent increase in running time over the minimum running times for a given precision in the determination of  $G_E$  and  $G_M$ . The values of  $MM_{\min}$  and  $ME_{\min}$  depend critically on the models used for the form factors, however, both the positions of the minima and the general shapes of  $ME(\theta)$  and  $MM(\theta)$  are relatively model independent and thus this approach is useful in designing our experiment.

2. **The values  $ME_{\min}$  and  $MM_{\min}$  are very insensitive to the value of the minimum angle at which the cross section is measured, provided this angle is less than 15 degrees.** Thus, the 8-BeV/c spectrometer can satisfactorily be employed to carry out the entire program of measurements of  $G_E$  and  $G_M$ .

3. **It takes a much longer time to measure  $G_E^2$  to the same accuracy as  $G_M^2$ .** This is indicated in Fig. 6 where the ratio  $ME_{\min}/MM_{\min}$  is plotted



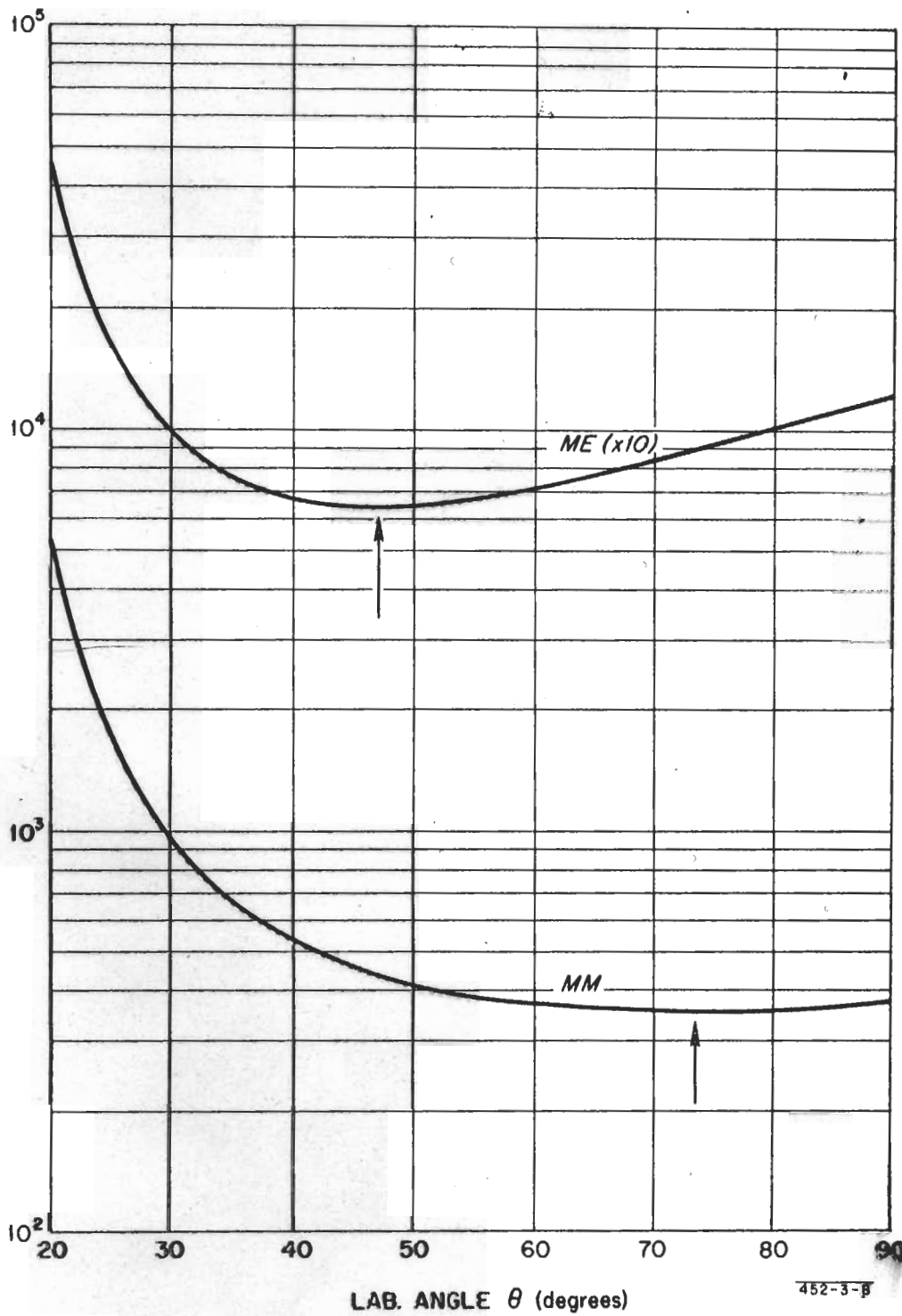


FIG. 3(a) - VARIATION OF ME AND MM FOR  $q^2 = 6.0(\text{BeV}/c)^2$

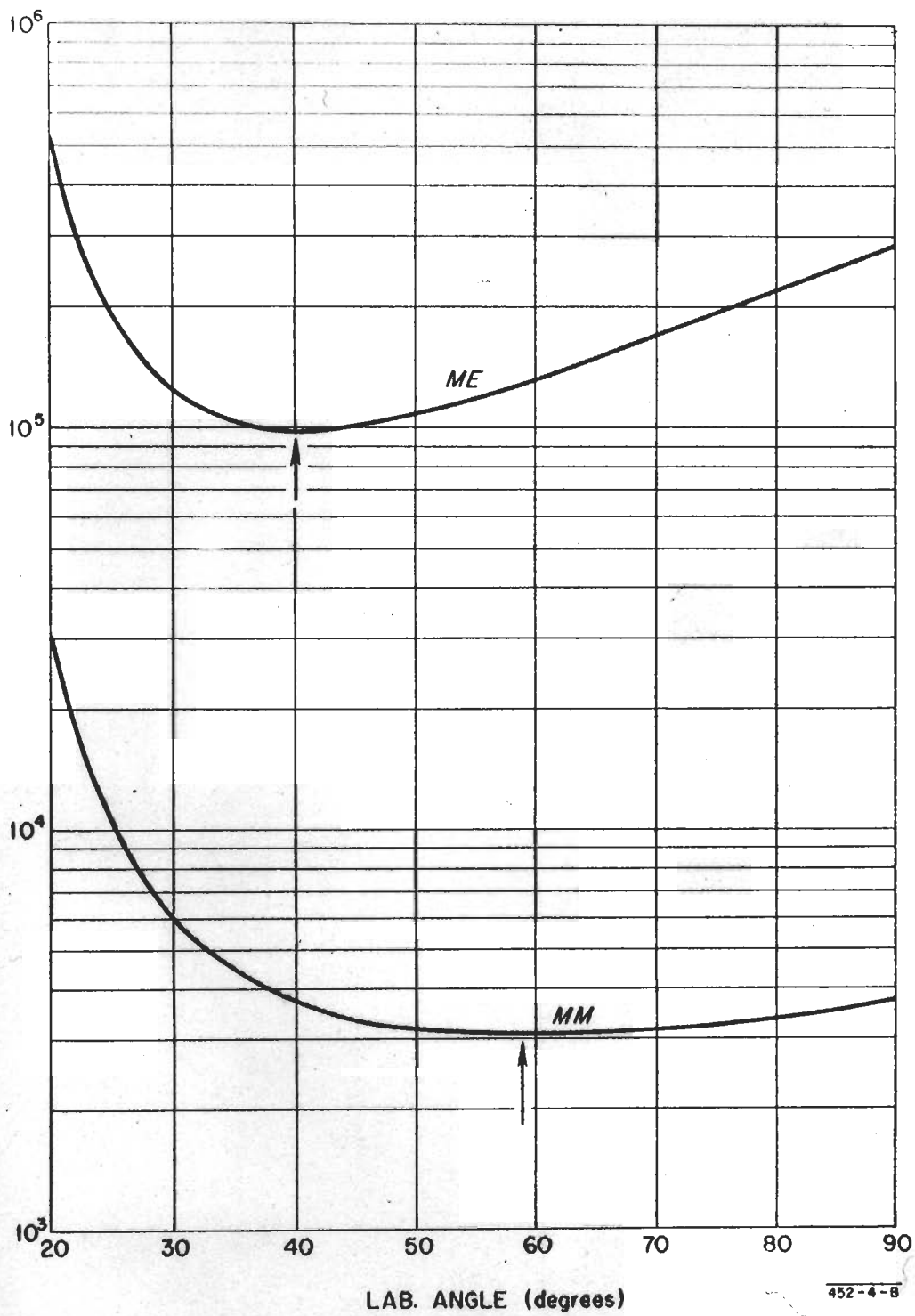


FIG. 3(b) - VARIATION OF ME AND MM FOR  $q^2 = 10.0 (\text{BeV}/c)^2$

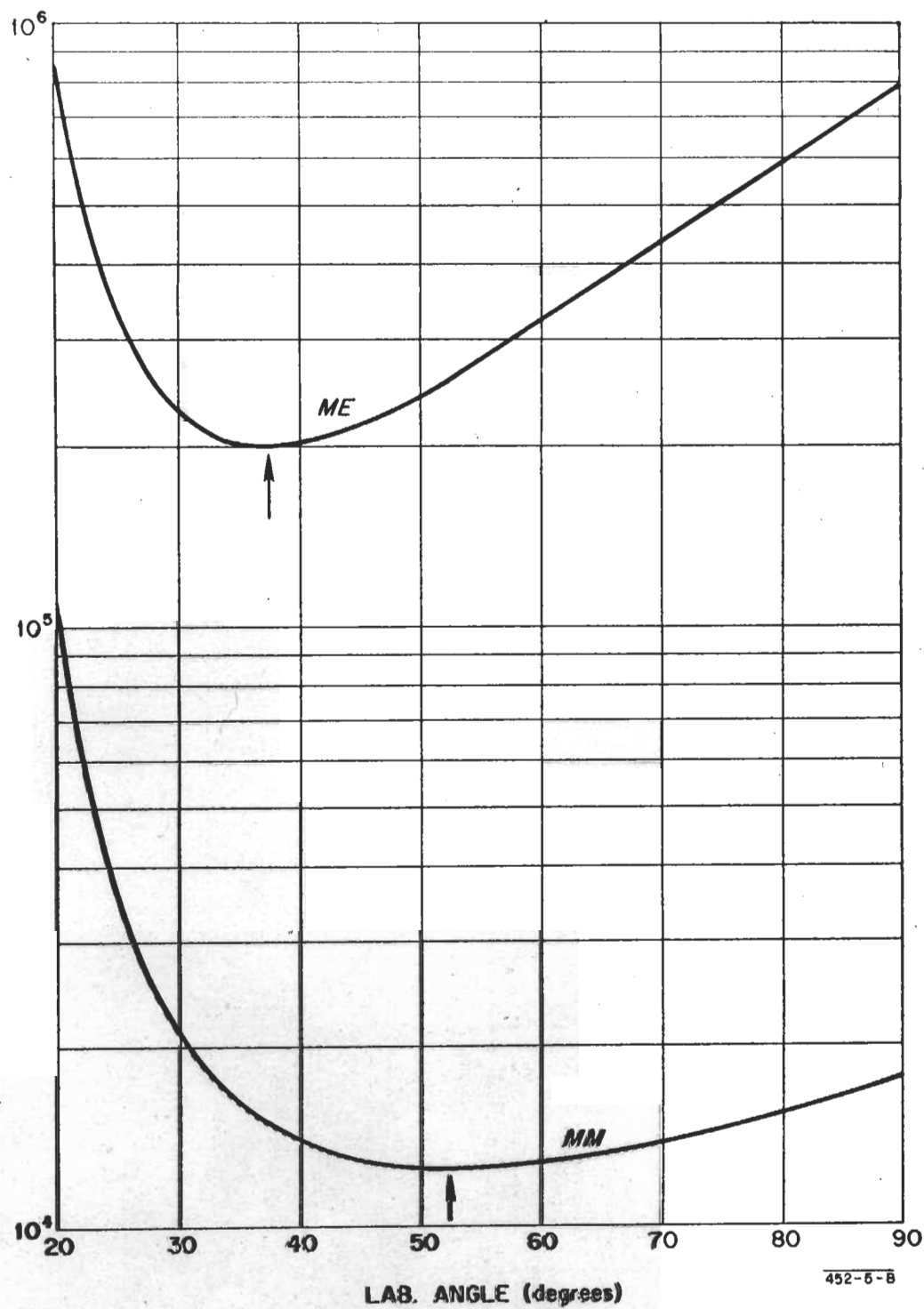


FIG. 3(c) - VARIATION OF ME AND MM FOR  $q^2 = 14.0(\text{BeV}/c)^2$



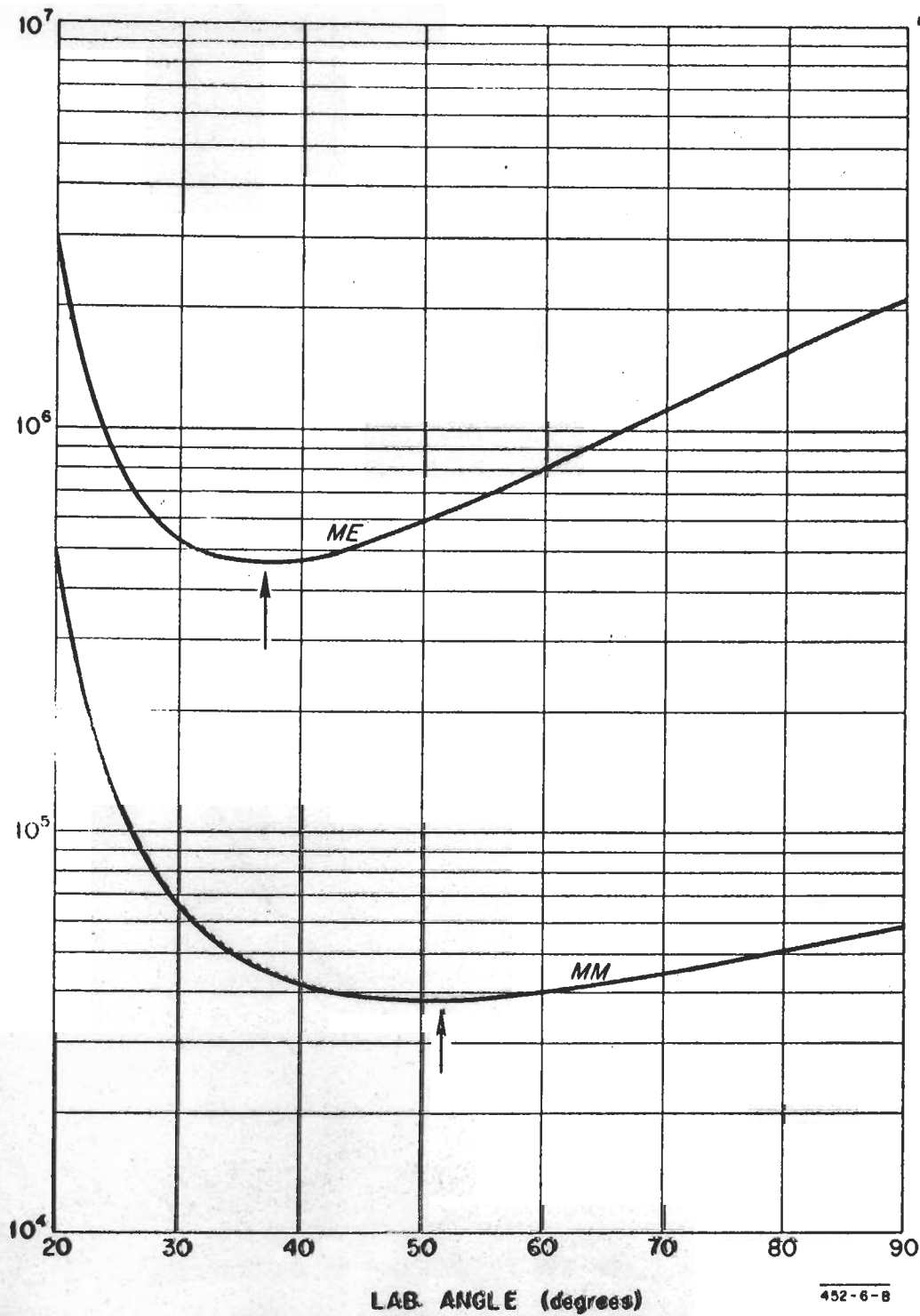


FIG. 3(d)-VARIATION OF ME AND MM FOR  $q^2 = 18.0(\text{BeV}/c)^2$

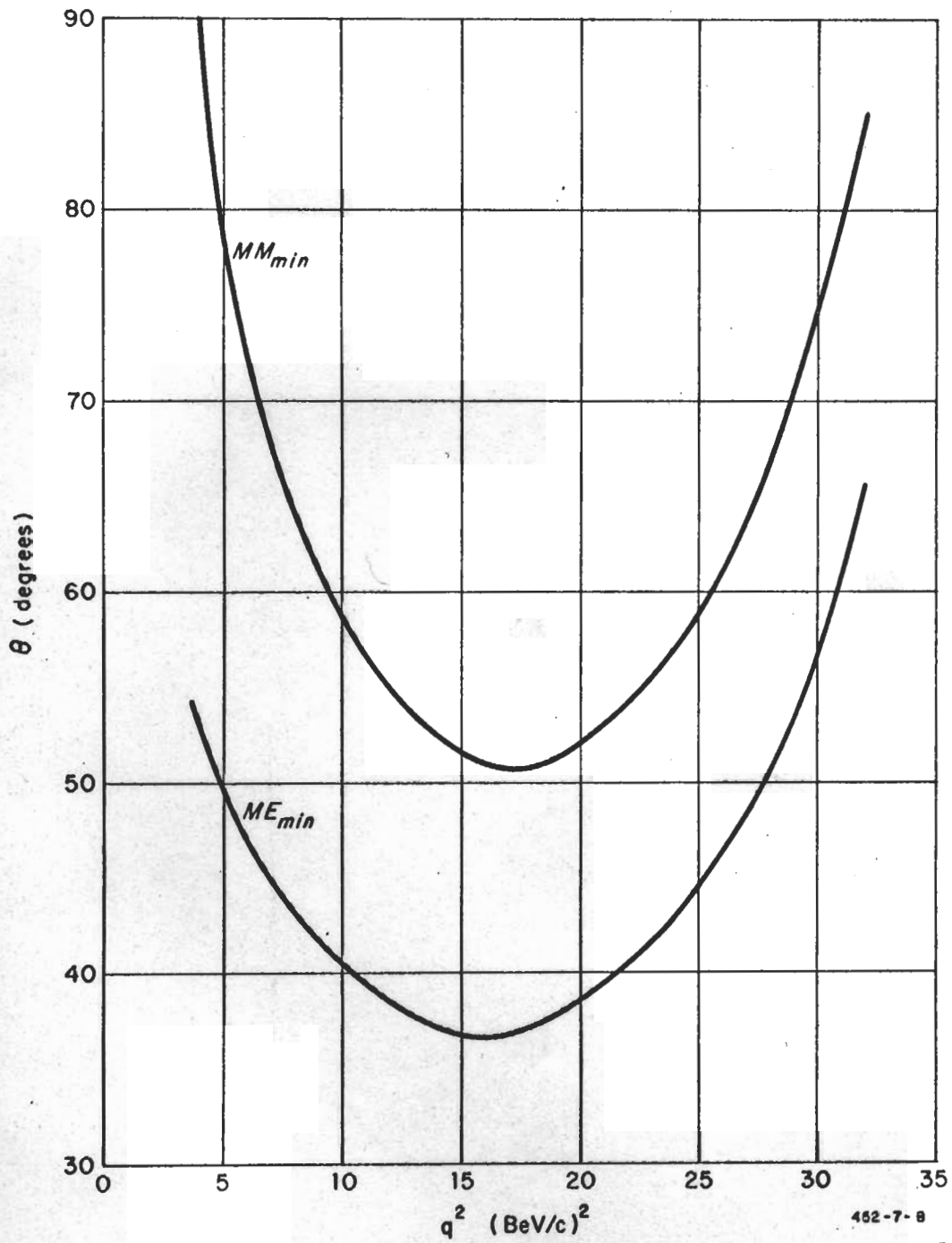


FIG. 4-VARIATION OF THE ANGLES FOR  $ME_{min}$  AND  $MM_{min}$  WITH  $q^2$

462-7-8

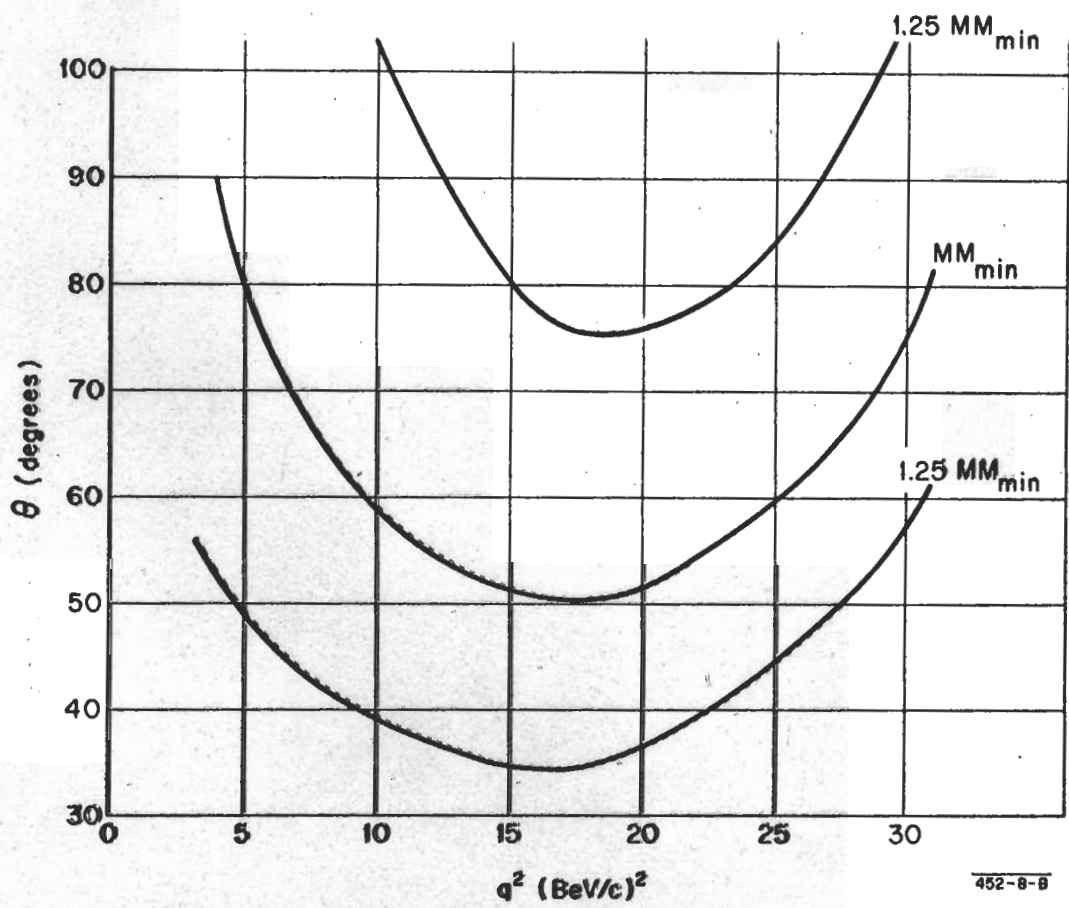
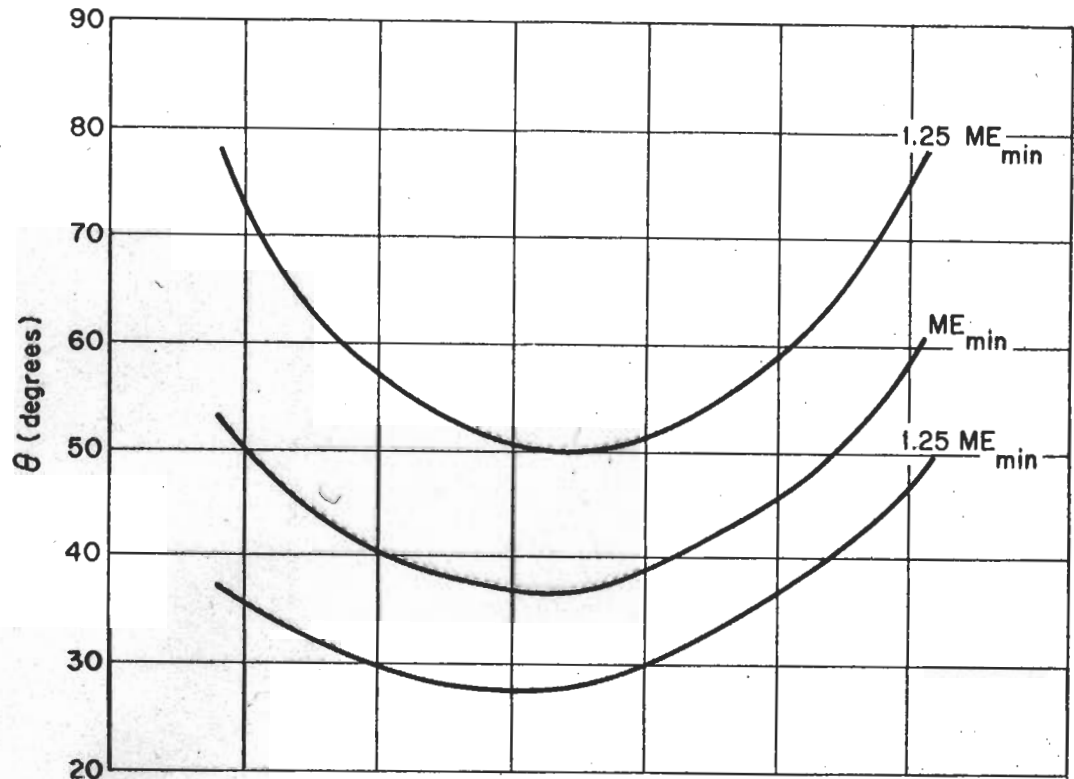


FIG. 5 - SENSITIVITY OF THE CHOICE OF ANGLES FOR  $ME_{\min}$  AND  $MM_{\min}$ .



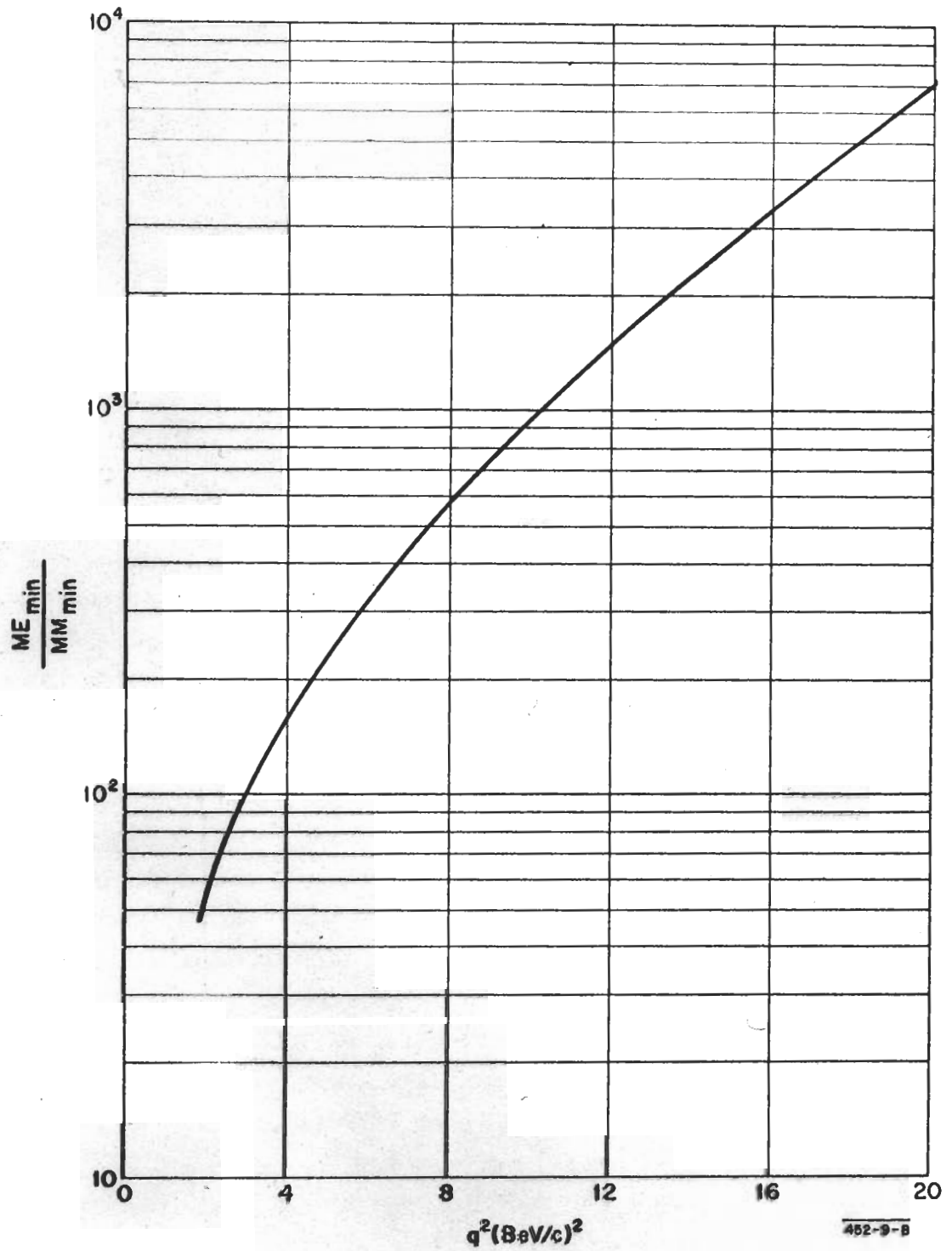


FIG. 6 - RATIO OF  $ME_{min}$  TO  $MM_{min}$  USING  $G_E = \frac{G_M}{\mu} = \frac{1}{\left(1 + \frac{q^2}{0.72}\right)^2}$

452-9-B

as a function of  $q^2$ . This calculation was based on the fit

$$G_E = G_M/\mu = \frac{1}{\left(1 + \frac{q^2}{0.72}\right)^2} .$$

Although one cannot take the numerical values of the ratio seriously because they depend strongly on the form factors being used, a strong trend is certainly indicated arising mainly from the dominance of  $\tau G_M^2/(1 + \tau)$  over  $G_E^2/(1 + \tau)$  in the intercept and the correlation of the errors in  $G_E^2$  and  $G_M^2$ .

#### E. Initial Objectives of Experiment

At the initial stages of this experiment it would be of great interest to learn the general features of the behavior of the form factors over a wide range of  $q^2$ . This would entail measuring the form factors with a limited precision up to fairly high four-momentum transfers. At the early stages, uncertainties about the behavior of the equipment will contribute to systematic errors which will decrease in magnitude as more information becomes available in the course of the experimental program. The predicted count rates for the experiment are strongly dependent upon the correctness of the expressions for the form factors. In spite of this uncertainty we present in Table I a "possible" set of runs based upon the  $d\sigma/d\Omega$  values given in Fig. 2. The angular ranges have been chosen assuming that the measurements are carried out in a manner which minimizes ME and MM (except for some cases where the ranges have been slightly reduced by the restrictions of the 8-BeV/c spectrometer).

The primary beam energy must be varied for each run at each angle and will range from 2.6 BeV at  $q^2 = 2.0$  (BeV/c)<sup>2</sup> and  $\theta = 42^\circ$ , to 16.5 BeV at  $q^2 = 16.0$  (BeV/c)<sup>2</sup> and  $\theta = 20^\circ$ . An arbitrary limit has been set at  $q^2 = 16.0$  (BeV/c)<sup>2</sup> as the predicted counting rates are down to about 4 events/hour, but this may be altered later when the actual rates are known. Thus, using the recent models of the form factors as a guide, we would expect that the program would allow a reasonable determination of  $G_M$  and a determination of an upper limit of  $G_E$  up to a  $q^2$  of about 16 (BeV/c)<sup>2</sup>. We may slightly extend this range to place a limit on  $G_M$  at higher  $q^2$  values (provided this region is not covered by Group F proposal using the 1.6-BeV/c spectrometer).

TABLE I  
A POSSIBLE RUN PROGRAM

$q^2$ (BeV/c) <sup>2</sup>	Range of Angles	Data Collection Time (hours)	Counting Statistics Errors Only			Predicted Range of Rates
			$\frac{d\sigma}{d\Omega}$	$\frac{\delta G_M^2}{G_M^2}$	$\frac{\delta G_E^2}{G_E^2}$	
2.0	12 - 42°	5	1%	4%	6%	10/sec (reduced intensity)
3.0		6				
4.0	14 - 50°	8	2%	7%	15%	5-1/sec
5.0		10				
6.0	16 - 45°	12	3%	11%	24%	60-4/min
7.0		15				
8.0	18 - 42°	20	5%	14%	35%	12-1/min
10.0		30				
12.0	19 - 38°	35	8%	25%	70%	120-15/hr
14.0		50				
16.0	20 - 37°	60	11%	34%	110%	30-4/hr

These calculated values are based on the CEA expressions for the form factors given in Ref. 1.

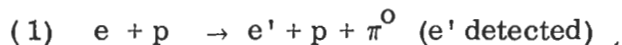


As the running time required to achieve these objectives depends on the exact behavior of the form factors we can only estimate the time. The program listed in Table I, for example, would require about 250 hours of actual data collection, but additional time would be needed for aligning the spectrometer at each angle of the 50 measurements ( $\sim 1/2$  hour each). Allowing about 75 hours for the initial checking out of the electronic system of the detectors and time for background investigation, it would thus seem reasonable to ask for a total of about 350 hours of running at  $2 \times 10^{13}$  electron/sec. This intensity has been used in the preparation of Table I, except for the lowest  $q^2$  points where the beam intensity must be decreased to avoid counting loss problems. This number corresponds approximately to the maximum design output of the accelerator at 360 cycles/sec into a primary beam energy spread of  $\sim \pm 0.1\%$ . As shown in Appendix II, this energy resolution is only required for a small number of the proposed measurements. At larger angles and lower primary energies it may be possible to open the BSY slits and obtain the required electron flux with either lower beam in the accelerator or a lower repetition rate.

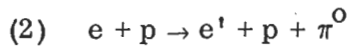
In view of the uncertainties associated with our estimate of the time required we expect, at the end of 200 hours of running, to submit a status report outlining what part of the program has been accomplished, what remains to be done, and a new estimate of the running time required based upon improved information.

#### F. Backgrounds

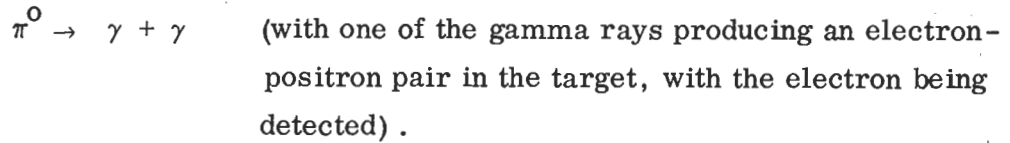
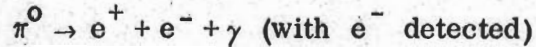
Use of the high resolution magnetic spectrometer and counter array for elastic scattering experiments provides conditions of very low background contamination. We list below the backgrounds which must be considered in evaluating the electron-proton elastic scattering experiment, although it is clear that they will not present any problem for these measurements.



The threshold for this process is 0.7% below the elastic peak at an incident energy of 20 BeV, and the separation for lower incident energies goes as  $(0.7\%) \times (20\text{-BeV}/E_0)$ . Since the full width at half maximum of the resolution function for this experiment is expected to be about 0.25%, the resolution of the system will be adequate to reject this background.



The neutral pion must decay by the following modes:



This process can give rise to electrons very close to the elastic peak; however calculations indicate that it is expected to be a small effect. This is shown in the following estimate. We can take

$$\left( \frac{d^2\sigma}{d\Omega dE'_{in}} \right)_{e+p \rightarrow e'+p+\pi^0} \approx (.02) \left( \frac{d\sigma}{d\Omega} \right)_{\gamma+p} \cdot \left( \frac{1}{E'_{el} - E'_{in}} \right)$$

where  $E'_{in}$ ,  $E'_{el}$  are the energies of electron having inelastically and elastically scattered, respectively. Measurements at CEA indicate that

$$\left( \frac{d\sigma}{d\Omega} \right)_{\gamma+p \rightarrow p+\pi^0}$$

is about  $10^{-32} \text{ cm}^2/\text{sr}$  at about  $25^0$  and 4 BeV in the laboratory, and is falling as a function of energy and angle. We will use this value for the estimate of the background. Because of the resolution of the detecting system, the  $\pi^0$  decay products can cause a detectable background only if  $0 \lesssim E'_{in} \lesssim 0.01 E'_{el}$ . Thus

$$\left( \frac{d^2\sigma}{d\Omega dE'_{in}} \right)_{e+p \rightarrow e'+p+\pi^0} \cdot \Delta E'_{in} \approx 2 \times 10^{-36} \text{ cm}^2/\text{sr}.$$

The probability that a Dalitz decay occurs is about 1/80. The fraction of phase space that allows the  $e^-$  from the decay to be detected must also be included. With these factors included the effective cross section for producing background electrons from this source is about  $\lesssim 10^{-40} \text{ cm}^2/\text{sr}$ . The calculation for  $\pi^0 \rightarrow \gamma + \gamma$  with one of the  $\gamma$ -rays interacting in the target to produce a pair yields about the same result.

(3)  $e + p \rightarrow e' + p + \pi^- + \pi^+$  (with detection of the  $\pi^-$ ).

Since  $\pi^-$  can only be produced from the proton as a member of a  $\pi$ -pair it is kinematically separated from the elastic peak and the resolution is adequate to reject this background.

(4)  $e + n \rightarrow e' + p + \pi^-$  (where the incident electron interacts with the target walls and the  $\pi^-$  is detected).

From the background contribution (2), we can estimate the effective cross section for producing  $\pi^-$  into the proper momentum range to be  $< 10^{-35}$  cm<sup>2</sup>/sr. Thus the yield of detected  $\pi^-$  as compared with electrons from elastic e-p scattering is given by:

$$\frac{Y_{\pi^-}}{Y_{e^-}} = \frac{10^{-35} \text{ cm}^2/\text{sr}}{\left(\frac{d\sigma}{d\Omega}\right)_{e+p \rightarrow e+p}} \cdot \frac{N'}{N} \frac{\epsilon_{\pi}}{\epsilon_e}$$

where  $N'$  is the number of neutrons/cm<sup>2</sup> in the target wall thickness, which we will take to be 2 mil of stainless steel,  $N$  is the number of protons/cm<sup>2</sup> in the target,  $\epsilon_{\pi}$  is the efficiency for detecting pions, and  $\epsilon_e$  is the efficiency for detecting electrons.

$$\frac{N'}{N} = \frac{4.9 \times 10^{22}}{8.4 \times 10^{23}} = 5.8 \times 10^{-2} \text{ (for a 20 cm liquid hydrogen target)}$$

and  $\epsilon_{\pi}/\epsilon_e \sim 10^{-4}$  is the expected order of magnitude of the  $\pi$  rejection by the  $\pi$ -e discriminator which is being constructed. Thus this background is not a problem since it makes a sizable contribution only where the e-p cross section falls below  $\sim 10^{-40}$  cm<sup>2</sup>/sr.

#### G. Radiative Corrections

The radiative degradation of the elastic peak arises from two different processes. In the first the incident and scattered electrons undergo bremsstrahlung in the target. The second consists of the emission of radiation during scattering. A correction is made for the first process by applying the results of the well-known



bremsstrahlung theory. The corrections for the second have been given both by Tsai<sup>(7)</sup> and by Meister and Yennie<sup>(8)</sup> for the case in which only the electron is detected. In addition to adding a low momentum tail to the elastic peak, these radiative effects decrease the size of the elastic peak. The measured and Rosenbluth cross sections are related by

$$\left(\frac{d\sigma}{d\Omega}\right)_{\text{meas.}} = \left(\frac{d\sigma}{d\Omega}\right)_{\text{Rosenbluth}} \cdot (1 + \delta_s), \quad \text{where } \delta_s < 0.$$

Figure 7(a) shows  $\delta_s$  as a function of the scattering angle for an incident electron energy of 20 BeV over the kinematic region covered by this program. Because the threshold for inelastic electron scattering occurs 0.7% down in momentum from the elastic peak for an incident energy of 20 BeV, we can only include about 0.5% of the radiative tail in measuring the cross section at this energy. Accordingly, in calculating  $\delta_s$  we use for  $\Delta E/E$  the value  $[0.007(20\text{-BeV}/E_{\text{inc}}) - 0.002]$ . From this figure and from the considerations of Appendix V we conclude:

(1) That the radiative effects do not seriously degrade the resolution of the elastic peak.

(2) That the depletion of the elastic peak is of the order of 30%. These calculations have included only contributions from the term  $\delta_s$  (which are of order  $\alpha$ ). Higher order corrections involving  $\alpha^2$  contributions will soon be published<sup>(9)</sup> and fairly accurate estimates of the radiative corrections will be made.

#### H. The Statistical Analysis Which Minimizes the Experimental Running Time

We here describe a simple statistical analysis which is used for the e-p elastic scattering experiment. The aim is to minimize the total accelerator time required to determine the form factors to given accuracies.

Suppose that we make measurements of the quantity  $y$  at  $N$  positions of  $x$  and try to make a least-squares fit of the data into a straight-line form:

$$y = mx + b.$$

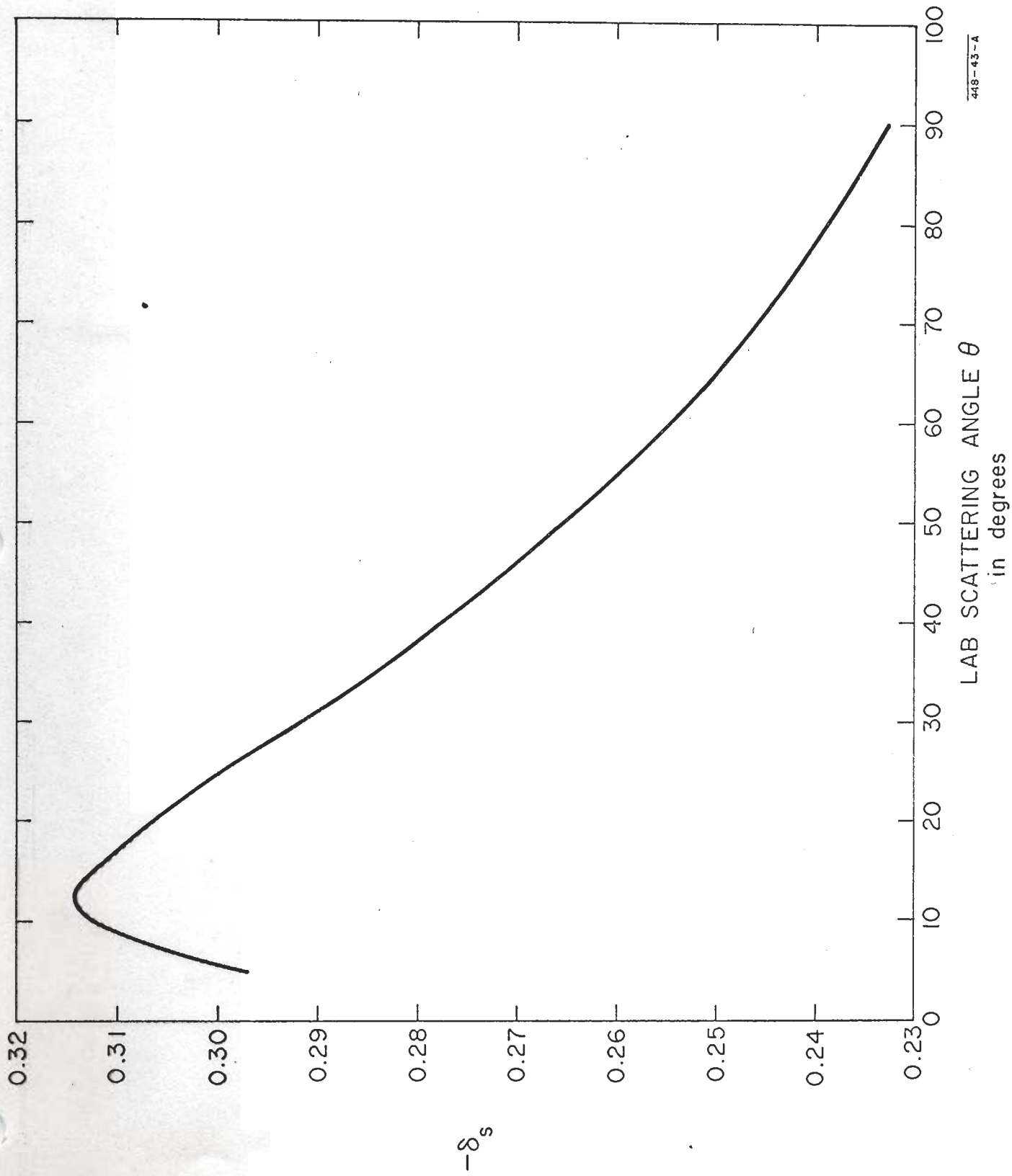


Fig. 7A--Radiative corrections for  $E_0 = 20$  BeV.

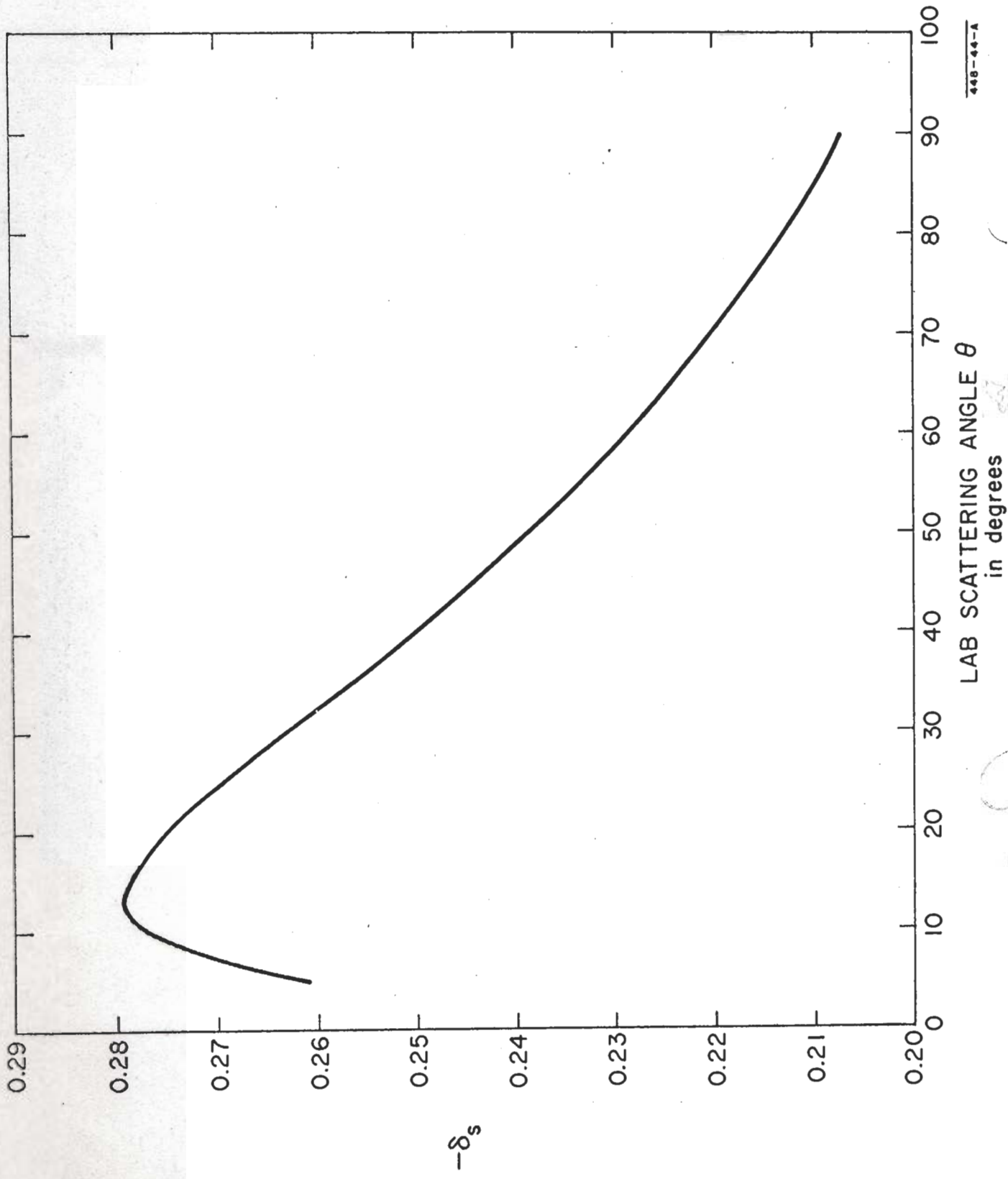


Fig. 7B--Radiative corrections for  $E_0 = 15$  BeV.



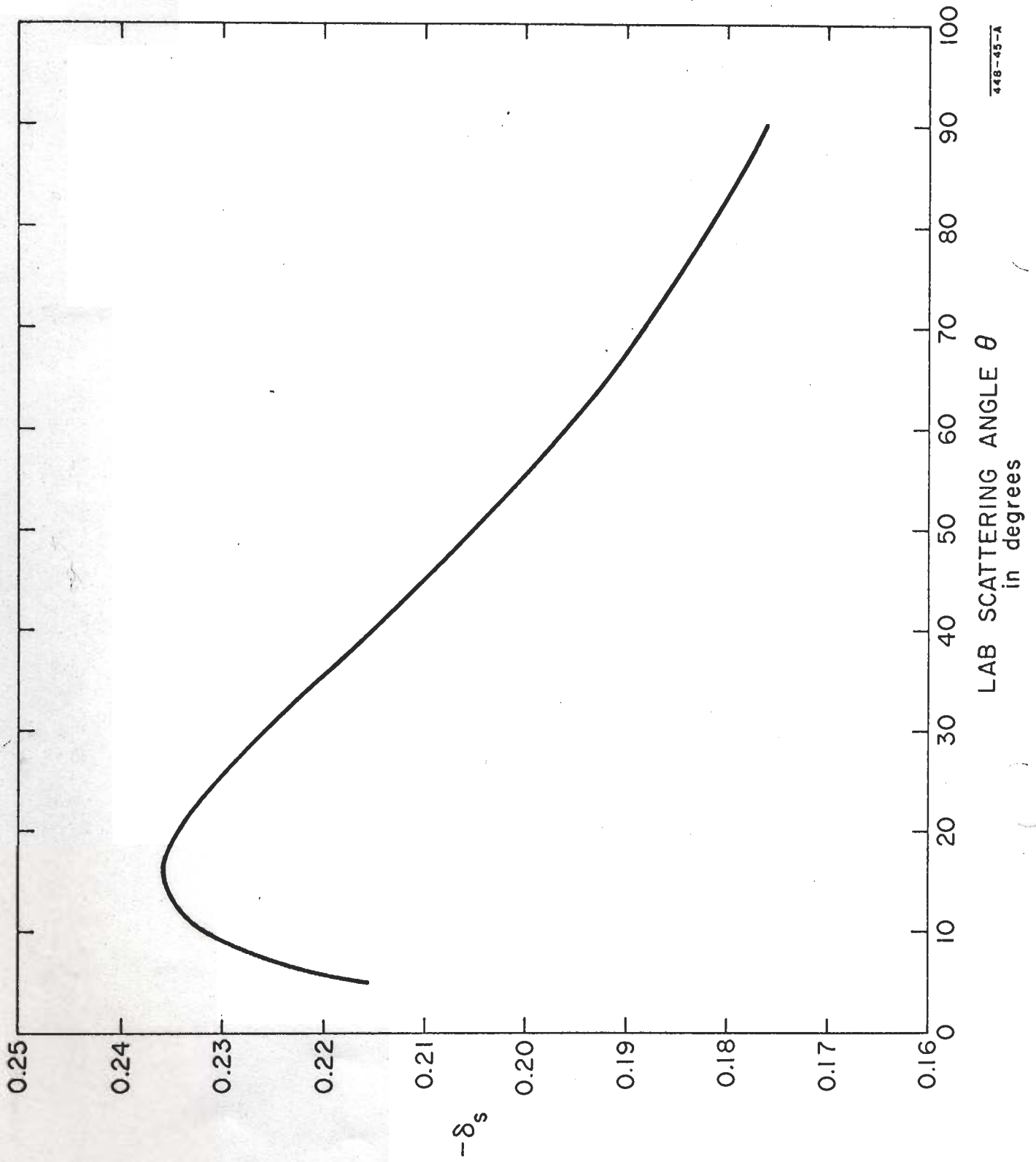


Fig. 7C--Radiative corrections for  $E_0 = 10$  BeV.

The square of the errors in the coefficients is given by

$$(\delta b)^2 = \frac{1}{\Delta} \left( \sum_i \frac{x_i^2}{\sigma_i^2} \right)$$

$$(\delta m)^2 = \frac{1}{\Delta} \left( \sum_i \frac{1}{\sigma_i^2} \right)$$

and the correlation between the errors is

$$(\delta b \cdot \delta m) = -\frac{1}{\Delta} \left( \sum_i \frac{x_i}{\sigma_i^2} \right)$$

where

$$\sigma_i = \text{error in } y_i$$

$$\Delta = \left( \sum_i \frac{1}{\sigma_i^2} \right) \left( \sum_i \frac{x_i^2}{\sigma_i^2} \right) - \left( \sum_i \frac{x_i}{\sigma_i^2} \right)^2$$

and the errors in  $x_i$ 's are assumed to be zero.

For the electron-proton elastic scattering experiment, the total number of counts is given by

$$N_i = K t_i \sigma_{NS} \left( \frac{G_E^2 + \tau G_M^2}{1 + \tau} + 2 \tau G_M^2 x_i \right)$$

where

$K$  = a constant which depends on the number of incident electrons per second, the target, and the solid angle of the instrument.

$t_i$  = counting time.

$x_i = \tan^2 \theta_i/2$  .

We can make the following identifications,

$$y_i = \frac{N_i}{K t_i \sigma_{NS}}$$

$$b = \frac{G_E^2 + \tau G_M^2}{1 + \tau}$$

$$m = 2 \tau G_M^2$$

$$\sigma_i = \frac{\delta N_i}{K t_i \sigma_{NS}} \quad .$$

Taking the point of view that the limiting error is systematic and that we count only until the statistical error is equal to the systematic error, then

$$\left( \frac{\delta N_i}{N_i} \right)_{\text{statistical}} = \frac{1}{\sqrt{N_i}} = \left( \frac{\delta N_i}{N_i} \right)_{\text{systematic}} = \epsilon_i$$

Assuming that there is no correlation between the statistical and the systematic error, we have

$$\begin{aligned} (\delta N_i)^2 &= (\delta N_i)_{\text{statistical}}^2 + (\delta N_i)_{\text{systematic}}^2 \\ &= 2 \epsilon_i^2 N_i^2 \end{aligned}$$

and

$$\sigma_i^2 = \frac{2 \epsilon_i^2 N_i^2}{K^2 t_i^2 \sigma_{NS}^2}$$

$$= 2 \epsilon_i^2 (m x_i + b)^2$$



We will consider the case in which all  $\epsilon_i = \epsilon$ . The counting time for each point is

$$t_i = \frac{1}{\epsilon^2 K \sigma_{NS} (mx_i + b)}$$

(1) The Magnetic Form Factor

The error in the magnetic form factor,  $G_M$ , is related to the error in the slope by the following expression

$$\begin{aligned} (\delta G_M^2)^2 &= \left(\frac{1}{2\tau}\right)^2 (\delta m)^2 \\ &= \frac{1}{\Delta} \left(\frac{1}{2\tau}\right)^2 \left(\sum_i \frac{1}{\sigma_i^2}\right) \end{aligned}$$

where  $\Delta$  is defined above and

$$\sigma_i^2 = 2(mx_i + b)^2 \epsilon^2$$

The total counting time for  $N$  points is given by

$$\begin{aligned} T &= \sum_{i=1}^N t_i \\ &= \sum_{i=1}^N \frac{1}{\epsilon^2 K \sigma_{NS} (mx_i + b)} \end{aligned}$$

If we divide the whole range of  $x$  into  $(N-1)$  equal intervals, we have

$$x_i = x_{\min} + (N_i - 1) d$$

where

$$d = \frac{1}{(N-1)} (x_{\max} - x_{\min})$$

We will define a figure of merit for measuring the magnetic form factor as  $1/MM$ , where

$$MM = \left( \frac{\delta G_M^2}{G_M^2} \right)^2 T$$

This figure of merit is independent of  $\epsilon$ , since  $(\delta G_M^2)^2$  is proportional to  $\epsilon^2$  and  $T$  is inversely proportional to  $\epsilon^2$ . It is thus possible to calculate the figure of merit  $MM$  using the above equations.

## (2) The Electric Form Factor

The electric form factor,  $G_E$ , is obtained from the intercept of ordinate by a subtraction. The intercept is

$$b = \frac{G_E^2 + \tau G_M^2}{1 + \tau}$$

From which we have

$$\delta G_E^2 = (1 + \tau) \delta b - \frac{1}{2} \delta m$$

$$(\delta G_E^2)^2 = (1 + \tau)^2 (\delta b)^2 + \frac{1}{4} (\delta m)^2 - (1 + \tau) \langle \delta m \cdot \delta b \rangle$$

$$= \frac{1}{\Delta} \left[ (1 + \tau)^2 \sum_i \frac{x_i^2}{\sigma_i^2} + (1 + \tau) \sum_i \frac{x_i}{\sigma_i^2} + \frac{1}{4} \sum_i \frac{1}{\sigma_i^2} \right]$$

where  $\Delta$  is defined above and  $\sigma_i^2 = 2 (mx_i + b)^2 \epsilon^2$ .

We will define a figure of merit for measuring the electric form factor as  $1/ME$ , where

$$ME = \left( \frac{\delta G_E^2}{G_E^2} \right)^2 T$$

This figure of merit which, is also independent of the counting error  $\epsilon$ , can thus be calculated using the above equations.

## REFERENCES

1. T. Janssens, R. Hofstadter, E. B. Hughes and M. R. Yearian, "Proton Form Factors From Elastic Electron-Proton Scattering," submitted to Phys. Rev., September 1965.  
K. Berkelman, M. Feldman, R. M. Littauer, G. Rouse, and R. R. Wilson, Phys. Rev. 130, 2061 (1963).  
J. R. Dunning, Jr., K. W. Chen, A. A. Cone, G. Hartwig, N. F. Ramsey, J. K. Walker and Richard Wilson, Phys. Rev. Letters 13, 631 (1964).  
See also: R. Hofstadter, Nuclear and Nucleon Structure (Benjamin, Inc. New York, 1963).
2. T. T. Wu and C. N. Yang, Phys. Rev. 137, B708 (1965).
3. S. D. Drell (private communication).
4. R. G. Sachs, Phys. Rev. Letters 12, 231 (1964).
5. A. Browman, F. Liu and C. Schaerf, Phys. Rev. 139, B1079 (1965).
6. L. H. Hand, D. G. Miller and Richard Wilson, Rev. Mod. Phys. 35, 335 (1963).
7. Y. S. Tsai, Phys. Rev. 122, 1898 (1961).
8. N. Meister and D. R. Yennie, Phys. Rev. 130, 1210 (1963).
9. D. R. Yennie (private communication).